Failure mechanisms of yarns subjected to ballistic impact

D. J. CARR
Defence Clothing and Textiles Agency, Science and Technology Division, Colchester, Essex, CO2 7SS, UK
E-mail: djcarr@dcta.demon.co.uk

Modern body armor and military helmets contain polymeric fibers. In body armor, these materials are usually used in the form of textiles, while in military helmets, textiles are reinforced with a polymeric matrix resulting in a composite construction. It is commonly accepted that the ballistic performance of a composite is approximately 30% less than for an unbonded assembly of the equivalent number of textile layers [1]. This results in a helmet that is significantly heavier per unit area for a given level of protection compared to a textile-only structure—for example, body armor. An understanding of the mechanisms of failure of these two different structures may, therefore, lead to a significant reduction in mass of a military helmet manufactured from a composite material and/or an increased protection at the same mass. Textiles and composites are complex structures; therefore, this work begins by considering single yarns.

The response of a number of para-aramid and ultra-high molecular weight polyethylene (UHMWPE) yarns to a ballistic impact was studied. The yarns studied are widely used in body armor and military helmets. The experimental procedures used were designed to allow the identification of both the major modes, and mechanisms, of failure. Of particular interest was the response of the virgin yarn material to a ballistic impact event and to characterize the effect of impact energy on the mode of failure. This was achieved by the use of a steel sphere of mass 0.68 g. The velocity of the sphere was manipulated to achieve different impact energies. The whole event was observed using a high-speed imaging system that allowed the failure mode to be observed. A post-failure analysis of the yarns allowed the identification of the failure mechanisms of the individual fibers and allowed a number of assumptions regarding the major energy absorbing mechanisms to be made.

The yarn materials used in this study are described in Table I. Para-aramid fibers are classified as aromatic polyamides. There are two major variants commercially available for use in fragment protective items: Kevlar (manufactured by Du Pont) and Twaron (manufactured by Akzo Nobel). UHMWPE fibers are manufactured by a gel-spinning process resulting in a material with a molecular orientation in excess of 95% and a high level of crystallinity (up to 85%). There are two variants of UHMWPE available for use in fragment protective clothing: Dyneema (manufactured by DSM High Performance Fibers) and Spectra (manufactured by AlliedSignal). Unfortunately, Spectra yarn is not available within the EU due to a licensing agreement between DSM High Performance fibers and AlliedSignal and was not, therefore, considered in this study.

A 0.68 g steel sphere was mounted in a nylon 6,6 sabot, which was placed in a 7.62 mm NATO capped cartridge case. The assembly was placed in a pressure housing and fired at the center of a single yarn, which was positioned at a distance of 3.46 m. The specimen length used for the testing was 0.57 m. A pair of optical timers positioned between the muzzle and the target detected the muzzle velocity of the sphere. The impact event was observed using a Hadland Imacon 468 high-speed imaging system. The flashguns and camera were triggered by an acoustic detector that was positioned at a distance of 0.31 m from the target. The whole system was controlled via a computer that served to display the captured image and was additionally used for image-processing activities. Fifty ballistic tests were completed at velocities ranging from 346 to 720 m/s. Ten tests were completed on each yarn type in ambient conditions of temperature and humidity.

The optical microscopes used were a Nikon KL150 stereomicroscope and a Leica DMR optical microscope. The yarns were observed unmounted. The microscopes were connected to a color video camera (JVC KY-F55B) and to a color video printer (Sony mavigraph). Scanning electron microscopy (SEM) was completed using an ElectroScan environmental SEM, or ESEM, which allowed the observation of non-conducting specimens without the requirement for a conducting layer. Such an arrangement ensures that delicate fracture surfaces are not disturbed. Typical examples of fracture

TABLE I Specimens considered

Yarn	Type	Linear density decitex*
Kevlar K129	Para-aramid	930
Kevlar KM2	Para-aramid	940
Twaron CT	Para-aramid	930
Dyneema SK66	UHMWPE	440
Dyneema SK66	UHMWPE	880

*Linear density (in tex) is the mass (g) per unit length (km) of the yarn.

© British Crown Copyright 1998/MOD
Published with the permission of the Controller of Her Majesty's Stationary Office

surfaces for each material were examined and recorded.

Failure occurred at the point of impact for all tests, indicating that the mounting system caused no edge effects. Two distinct major failure modes were observed in both para-aramid and UHMWPE yarns. The first of these was a transmitted stress wave (TSW) failure mode (Fig. 1). The second mode of failure appeared to be a shear or "plug" failure (Fig. 2). These modes of failure are typical of those observed in other materials [2].

An analysis of the impact energy required to

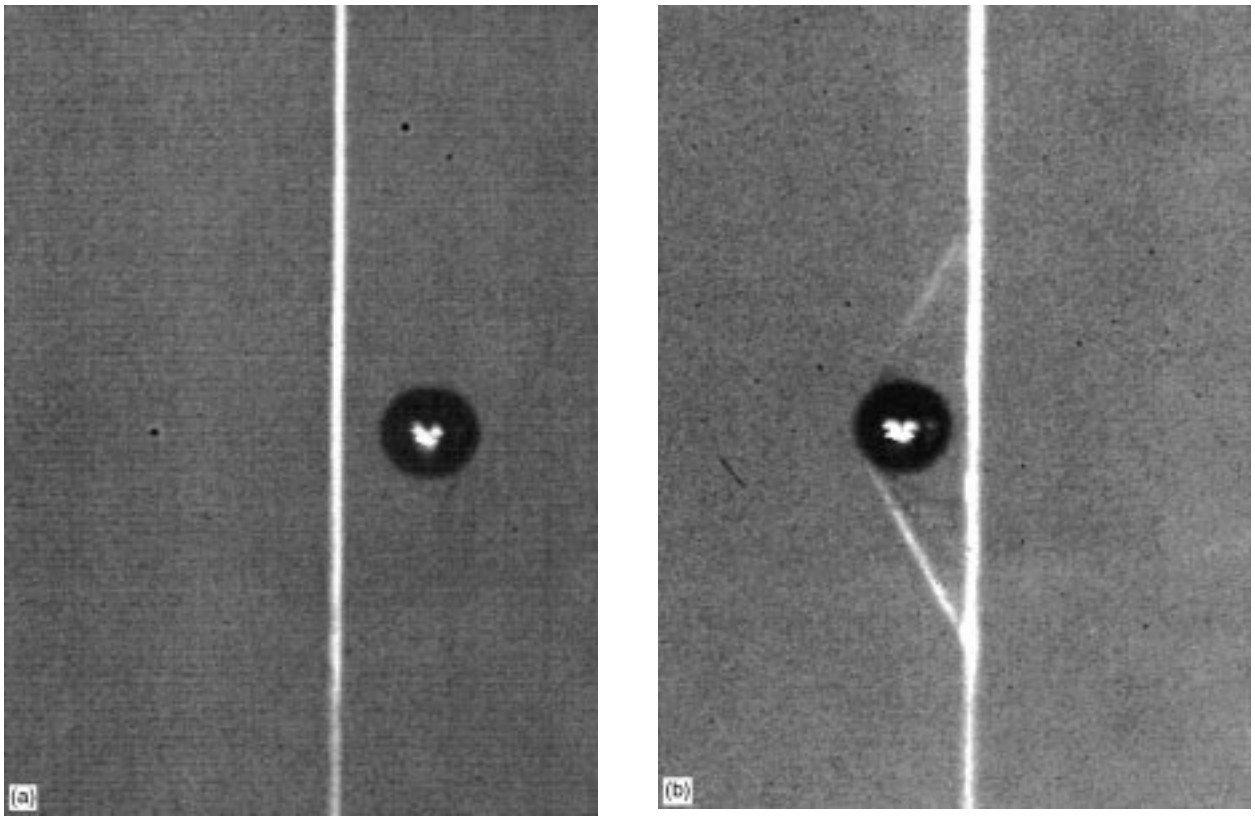

Figure 1 TSW failure mode.

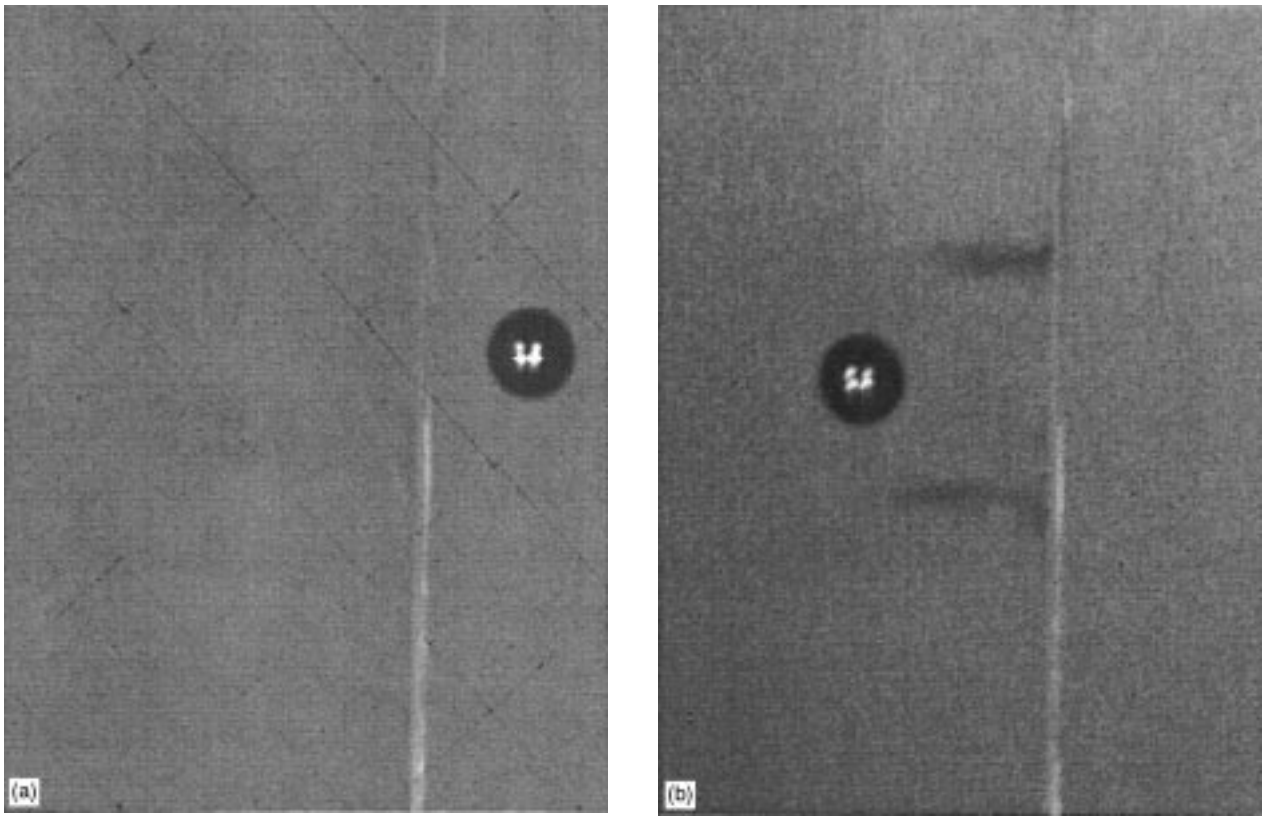

Figure 2 Shear failure mode.

produce either failure mode was completed on the fifty high-speed images obtained. The impact energy was calculated from the sphere mass and initial velocity. A critical impact energy was identified for each material type, which defined the transition between failure by TSW or by shear mode. For a para-aramid yarn, this transition occurred at approximately 130 J. For UHMWPE yarn, the transition between the TSW and shear modes was approximately 160 J.

The residual velocity of the sphere after penetration of the yarn was determined using the image-processing capabilites of the high-speed imaging system. The measurement of this velocity enabled the determination of the energy absorbed by the yarn during the impact event (assuming conservation of energy). The data obtained are presented in Fig. 3 and are expressed in terms of the specific energy absorbed, that is, energy absorbed by the yarn divided by the linear density of the yarn, versus the impact energy. Considering the different types of yarn, it appears that UHMWPE yarns absorb more energy than para-aramid yarns during ballistic impact, particularly at high-impact energies, which result in a shear mode failure. For para-aramid yarns, it appears that a low-impact energy resulted in an increased level of energy absorbed when compared to a high-impact energy. For UHMWPE yarn, however, the opposite appeared to occur, that is, a high-impact energy resulted in an increased level of energy absorbed compared to a low-impact energy.

The impact event resulted in a gross permanent disruption of the yarn structure for a distance of approximately 40 mm in all specimens. Microscopic examination of the impacted samples identified a number of pertinent features dependent upon material and failure mechanism.

Individual para-aramid fibers failed by fibrillation during both TSW and shear failure modes (see, example, Fig. 4). No significant differences in failure mechanism were observed for the three types of para-aramid fiber considered. It appeared that an increased degree of fiber fibrillation occurred during TSW failures. The production of this increased fracture surface area may account for the increased energy absorption observed when this material failed via a TSW mode compared to a shear failure mode.

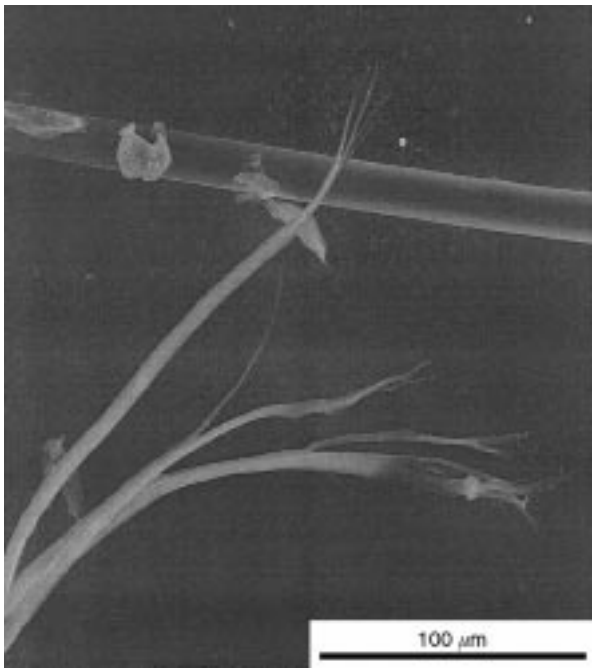

Figure 4 Fibrillation of aramid fibers.

At high-impact energies, it appeared that the more brittle nature of the material leads to a transverse rather than a longitudinal dominated fracture.

Fibrillation was not observed in UHMWPE fibers. For the TSW mode, shear failure of the fibers was observed (Fig. 5). In UHMWPE yarn shear mode failures, the fiber fracture surface appeared as a shear zone and was accompanied by shear bands in the adjacent region. At higher magnifications, a degree of melt damage was observed (Fig. 6). The formation of shear bands and melt damage may lead to the increased level of energy absorption observed in shear failures of UHMWPE yarn compared to UHMWPE TSW failures.

In conclusion, polymeric yarns were seen to fail in either a transverse stress wave mode (low-impact energies) or a shear mode (high-impact energies) when subjected to ballistic testing. For the para-aramid yarns studied, a low-impact energy resulted in increased energy absorption compared to a high-impact energy. Para-aramid fiber failure was by fibrillation in all tests; however, an increased level of fiber fibrillation was observed at low-impact energies

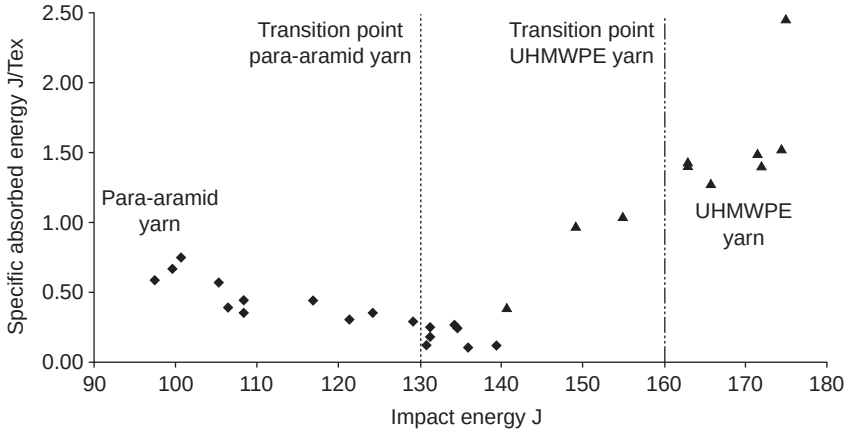

Figure 3 Specific absorbed energy versus impact energy for single yarns.

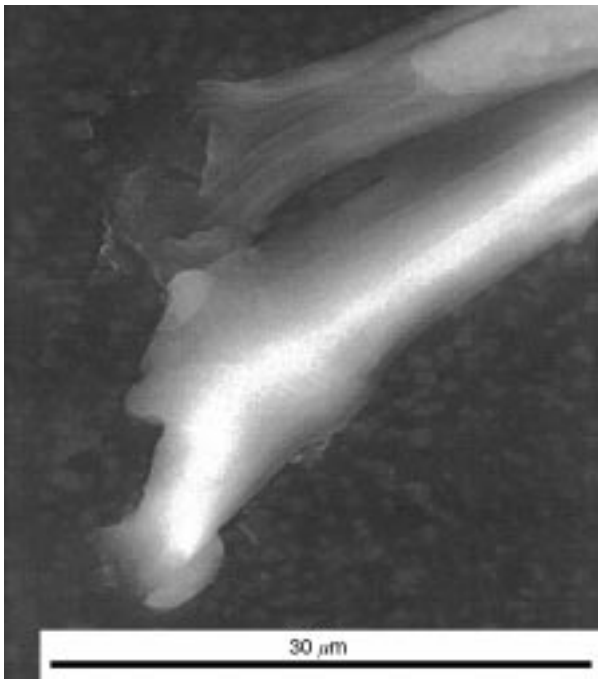

Figure 5 Shear failure—UHMWPE fiber.

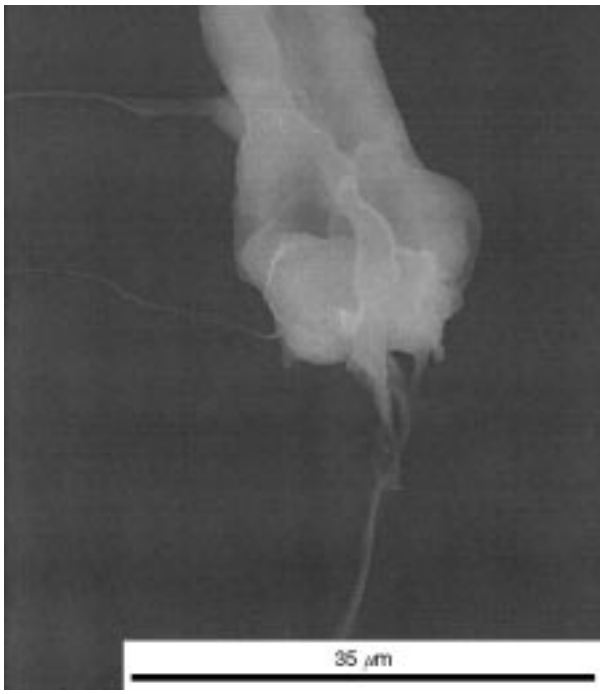

Figure 6 Melt damage—UHMWPE fiber.

compared to high-impact energies. For the UHMWPE yarn considered, a high-impact energy resulted in an increased level of energy absorption compared to a low-impact energy. At low-impact energies, individual fibers were seen to fail in shear. At higher impact energies, fiber melting and the formation of shear bands were observed.

Acknowledgments

The author would like to acknowledge and thank Mr. N. Wallis, who completed the ballistic tests referred to in this letter, and Professor I. Ward for his encouragement for the completion of this project. This work was funded through the DCTA innovative-corporate research program.

References

1. R. G. SHEPHARD, in "Polymers in defence" (The Plastics and Rubber Institute, London, 1987) p. 21/1.
2. J. HARDING, in "Materials at high strain rates", edited by T. Z. Blazynski (Elsevier Applied Science, London, 1987) p. 133.

Received 12 March
and accepted 15 July 1998